J Nanopart Res (2021) 23:106
https://doi.org/10.1007/s11051-021-05218-0

RESEARCH PAPER

Lipid nanoparticles for the transport of drugs like dopamine through the blood-brain barrier

Elena Ortega · Santos Blanco · Adolfina Ruiz · María Ángeles Peinado · Sebastián Peralta · María Encarnación Morales

Received: 8 March 2021 / Accepted: 20 April 2021

Abstract Diseases and disorders of the nervous system, like Parkinson disease (PD) and other neurodegenerative pathologies, are widespread in our society. The arsenal of treatments against these pathologies continues to increase, but in many cases, its use is limited. This is due to the blood-brain barrier (BBB), which acts by limiting the penetration of drugs into the brain. To overcome this handicap, in the current research, solid lipid nanoparticles (SLNPs) able to encapsulate drugs and to cross the blood-brain barrier have been designed to transport and release these drugs into their targets. These SLNPs were synthesized by a sonication method and high agitation process searching the most adequate physicochemical profile to achieve the objectives set. Today, the most efficient treatment for PD consists of providing the dopamine (DP) that is lost by neurodegeneration; however, the nature of this neurotransmitter prevents its crossing of the BBB. Therefore, DP may be considered as a good candidate to be encapsulated in SLNPs while studying how the loading drug could affect such nanoparticles. Based on these antecedents, in this research, both empty and DP-charged SLNPs were characterized physicochemically. The results obtained indicated a great stability of the nanoparticles loaded with DP when drug was used at 0.2 to 0.05%; these concentrations barely affected its size, polydispersity, and ζ-potential, and the SLNPs elaborated in this research were high appropriate to be injected systemically. Finally, empty SLNPs labeled and administered systemically to adult male Wistar rats demonstrate their penetration ability into the brain parenchyma.

Keywords Dopamine · Nanoparticles · Brain–blood barrier · Neurodegenerative diseases

E. Ortega · A. Ruiz · S. Peralta (✉) · M. E. Morales
Department of Pharmacy and Pharmaceutical Technology, School of Pharmacy, University of Granada, Campus de Cartuja s/n, 18071 Granada, Spain
e-mail: seperaltag@gmail.com

S. Blanco · M. Á. Peinado
Department of Experimental Biology, University of Jaén, Building B3, Campus de Las Lagunillas s/n, 23071 Jaén, Spain

Introduction

Neurodegenerative diseases represent a major issue in our society, so the development of novel strategies aiming to achieve effective methods for their treatment is crucial. Although many treatments are being developed constantly, many of them face difficulties in reaching their therapeutic targets, mainly due to the blood-brain barrier (BBB), an effective obstacle for many of the drugs designed to act on the central nervous system (CNS). In fact, when these drugs are administered, they first must go through the cerebral capillary endothelium formed by polarized endothelial cells highly glued to each other by tight connections. They also must cross the astroglial barrier, the pericytes, and in some cases even the perivascular mast cells (Masserini 2013). In addition, a large quantity of molecules, although may cross the BBB, they have a low rate of permeability showing difficulties to reach the nervous

Published online: 29 April 2021

parenchyma (Rehman et al. 2013; Pardridge 2015). Particularly, most hydrophilic molecules fail to cross the BBB because of the tight connections between cells, which limits transport (Niu et al. 2019). In fact, 98% of the potential drugs that could improve the treatment of many CNS diseases are not actually effective because of their inability to cross the BBB (Pardridge 2012).

To overcome these difficulties, nanoparticles (NPs) have been designed with materials that achieve the purpose of crossing the BBB. Among these materials, chitosan stands out as a cationic polymer that provides positive charge to NPs while also being biodegradable, biocompatible, and non-toxic (Naskar et al. 2019); in addition, surfactants have a fundamental role in the biosynthesis of these NPs, given that they are responsible for determining their structure. Polysorbate 80 (Tween® 80) facilitates endocytosis, since once it is adsorbed on the surface of the NPs, it is able to bind to apolipoprotein E (apoE), a membrane receptor substrate of the LDL protein (Tian et al. 2018). Finally, one of the main lipids contributing to the biosynthesis of NPs is glycerol tripalmitin; it is classified as "Generally Recognized as Safe" (GRAS) because it is a physiological type of lipid (Kakadia and Conway 2015). Therefore, the synthesis of drug-carrying lipid NPs synthetized from these materials offer many advantages, some of which are their low cost, high drug loading in comparison with others types of NPs, controlled released, simple synthesis, and the possibility of an intravenous administration with a constant release of the drug, which allows a possible reduction of side effects and reduction in the frequency of administrations. In fact, these types of NPs have the ability to cross the BBB and release the drug in the nervous parenchyma (Kuo and Rajesh 2018; Alyautdin et al. 2014).

There are various methods of NP preparation, including solvent injection, supercritical fluid technology, droplet-phase aerosol synthesis, microemulsion, membrane contactor method, and high-pressure homogenization among others (Ghasemiyeh and Mohammadi-samani 2018). In choosing a method for the preparation of NPs, the best option should as much as possible to avoid degradation of the drug and be easily reproducible. Following these objectives, we have used a nanoemulsion by ultra-sonification and high agitation method for the preparation of our NPs. This method is one of the most efficient approaches to preparing nanoemulsions due to the possibility of providing a high amount of energy locally through cavitation (Kumar et al. 2018).

We decided to complete the study by encapsulating dopamine (DP) in these NPs. In fact, DP is an ideal candidate in the development of a pharmaceutical form that allows drugs unable to cross the BBB reach the brain parenchyma and subsequently release an adequate dose of the drug while also protecting it and preventing its degradation (Pahuja et al. 2015).

Parkinson's disease (PD) is one of the most common neurodegenerative pathologies, and its most frequent treatment is to administer L-Dopa (DP precursor) because DP, as it has been mentioned, is unable to cross the BBB. L-Dopa is capable of crossing the BBB through a specific brain transport (6); once L-Dopa is located inside the brain parenchyma, a L-amino acid decarboxylase converts L-Dopa into DP. The great advantage of L-dopa is that it can go through the BBB and reach neurons. However, it has some disadvantages such as the loss of efficacy over time, sensitivity to oxidation, and the appearance of extrapyramidal symptoms like nausea or dyskinesia related to the metabolism of L-dopa outside the central nervous system (Trapani et al. 2011). Other alternatives for the treatment of PD consist in preventing the degradation of DP, but this option does not represent a long-term solution due to the effect of the neuronal degeneration progress (Zhou et al. 2018). These approaches aim to increase DP levels or regulate the synthesis of another neurotransmitter that influences motor symptoms. In fact, some drugs may improve DP levels in the brain in two ways: first, as DP precursors and second, by inhibiting enzymes that prevent the recapture of the DA (Ellis and Fell 2017).

Based on this background, the objective of this study was the design and development of solid lipid nanoparticles (SLNPs) capable of transporting different therapeutic molecules to the cerebral parenchyma affected by neurodegenerative diseases. The elaboration process was developed, and once prepared, the NPs were analyzed and physicochemically characterized. In addition, due to the prevalence of PD, one of the best drugs that could be used to treat this pathology would be DP; however, due to its nature, DP is unable to reach its therapeutic targets. So, we have encapsulated the DP inside of these SLNPs and we have studied them to ascertain if this SLNPs loaded with DP retain the same physicochemical properties as the empty ones. Finally, the empty SLNPs were marked and injected

systemically into control animals to demonstrate its ability to cross the BBB and reaching the brain cells successfully.

Material and methods

Materials

Dopamine hydrochloride (DP), Octadecylamine (OA), Glycerol Tripalmitin (GT), and Chitosan (CS) (low molecular weight) were purchased from Sigma-Aldrich Quimica SL (Madrid, Spain); Tween® 80 were obtained from Guinama (Valencia, Spain). Rhodamine-123, 2,3,5-Triphenyltetrazolium chloride, and PBS were obtained from Sigma-Aldrich Quimica SL (Madrid, Spain). Dichloromethane (DCM) was purchased from VWR (Barcelona, Spain), ketamine (Imalgene 100 mg/ml) from Merial Laboratorios S.A., and xylacine (Rompun®) from Bayer. Uranyl Acetate was obtained from Electron Microscopy Sciences (Hatfield, PA, USA), and distilled water was prepared by a Millipore (Billerica, MA, USA) system.

Synthesis of SLNPs

SLNPs were prepared according to a sonication method followed by the use of the high-speed homogenizer Silent Crusher-M from Heidolph. In a first step, an aqueous phase and an oily phase were mixed. On the one hand, the aqueous phase was composed of 7.5 ml of Tween® 80 solution (0.20 % w/v), 7.5 ml of CS solution (0.05 % w/v), and 10^{-4} M rhodamine but only in the empty SLNPs. In the case of NPs loaded with DP, it was used different concentrations of DP elaborated from an initial solution, reaching concentrations of (0.2 to 0.03 mg/ml). On the other hand, the oily phase was composed of GT (0.35 % w/v), OA (0.134% w/v), and 1ml of DCM.

The union of both phases is subjected to sonication during 6 min in parameters of 30 duty cycle and 3 out of control. Subsequently, it was subjected to agitation on a Silent Crusher M stirrer at 5500 rpm for 10 min.

Once elaborated, the DCM is eliminated by evaporation in a laminar flow hood at room temperature.

Characterization of SLNPs

Particle size, polydispersity index (PDI), and Zeta Potential (ζ-potential) measurement

The size and PDI of the SLNPs were determined by means of dynamic light scattering with Non-invasive Backscattering Optics (NIBS). For this, the mean particle size was determined by Malvern Zetasizer Nano ZS® (Malvern Instruments Ltd, Malvern, UK), at 25.0°C ± 0.5°C. The average size is expressed in nanometers (nm).

The measurement of ζ-potentials has been carried out in the same device (Malvern Zetasizer Nano ZS®; Malvern Instruments Ltd, Malvern, UK) using electrophoretic light scattering and a molecular weight analyzer with static light scattering. The colloidal dispersion is introduced partially diluted. ζ-potential is expressed in millivolts (mV).

In both cases, Malvern Instruments software was used; this software adapts automatically to the attenuation of the dispensing. Three measurements of each sample were made. These three measurements are the average among 10 to 15 repetitions depending on the sample.

Microphotographic analysis

SLNPs are arranged in the suitable supports (grids) for viewing under microscopy. The devices used for this study have been transmission electron microscope (TEM): CARL. ZEISS LEO 906E and Scanning Electron Microscope (SEM): Hitachi S-510. The Scientific Instrumentation Center (CIC) of the University of Granada (Spain) has facilitated both microscopes.

For TEM, the sample was prepared via negative staining. The dispersion was incubated in a grid with carbon support film for 5 min in a Petri dish and contrasted with 1% uranyl acetate in aqueous solution.

For SEM, a drop of the colloidal dispersion of SLNPs was deposited on a corresponding support for the FESEM (pin stub mount) allowing it to dry at room temperature. Subsequently, they were sputtered with carbon with Carbon Coater (Polaron CC7650).

Determination of drug encapsulation efficiency

To determine the efficiency of encapsulation performance of NPs, the dispersion was centrifuged using a centrifuge (Eppendorf AG 5804—Hamburg) at 14000 rpm for 20 min until we got a solid precipitate. The drug content in the supernatant was analyzed spectrophotometrically at 280 nm using a UV–VIS spectrophotometer (UV-Vis Perkin Elmer Lambda 25) against the blank.

The encapsulation was determined using the following formula:

Encapsulated percentage = (Actual drug content/theoretical drug content) × 100.

In vitro drug release study

In vitro drug release study was performed using a dialysis membrane (2 kDa molecular weight cutoff Spectra/Por® 6) containing 25 mL of pH 7.4 phosphate buffer. About 5 mL of SLNP dispersion was placed in the dialysis membrane, and both ends were sealed with magnetic weighted closures (Spectra/Por Clousures®). Then, the dialysis bag was kept in the receptor compartment containing dissolution medium (pH 7.4 phosphate buffer) at 37°C ± 0.5°C, which was stirred at 100 rpm for 168 h.

At regular time intervals, 1-ml samples were withdrawn and replaced with freshly prepared pH 7.4 phosphate buffer. The drug contents in the samples were analyzed spectrophotometrically at 280 nm by using a UV-VIS spectrophotometer (UV-Vis Perkin Elmer Lambda 25) against the blank.

In vitro drug release kinetics

Different mathematical models were tested to choose the one, which most reliably explains the release kinetics. Data was analyzed according to zero-order kinetics, first-order kinetics, Higuchi and Hixson Crowell models to search the model that best explains the diffusion process (Doménech Berrozpe et al. 2013); therefore, the Akaike Information Criterion (AIC) allows us to find the function that more accurately fits to the drug release process (Portet 2020). The criterion identifies the model that best fits the data as the one with the minimum value of AIC and was calculated applying the following equation:

$$AIC = n \cdot \ln SSQ + 2p$$

n number of pairs of experimental values
ln Neperian logarithm
SSQ sum of residual squares
p number of parameters of the adjustment function

The model that best fits the data was that with the lowest AIC.

Stability study

A solution of DP in water 0.034mg/mL was prepared. Three aliquots were taken:

A: It was kept at 4°C and in the absence of light.
B: It was kept at 25°C and in the absence of light.
C: It was kept at 25°C and in the presence of light.

All aliquots were measured 24 h and 1 week after their preparation. It was analyzed spectrophotometrically at 280 nm by using a UV-VIS spectrophotometer (UV-Vis PekinElmer Lambda 25) against the blank.

Experimental animals

The in vivo experimental procedures to assess the penetration of the empty SLNPs (eSLNPs) in the brain have been developed in adult male Wistar rats (Charles River). All procedures have been carried out in the Centre for Animal Production and Experimentation of the University of Jaen (CPEA) and previously approved by the local Animal Care Committee and performed in compliance with the Spanish legislation and in accordance with the EU Directive 2010/63/EU (2010).

Histology and microscopy

Histology and confocal microscopic analysis were carried out in the Research Support Services of the University of Jaén (SCAI).

To assess the efficiency of uptake of eSLNPs into the brain parenchyma, rhodamine-123-fluorescence-labeled-eSLNPs, prepared following the sonication method previously described, were injected in the animals throughout the radial tail vein. After 2h from the systemic NPs injection, animals were sacrificed; the brains were removed and cut into slices of 20 μm with a

cryostat (Leica CM1950). Then, slices were washed twice in phosphate-buffered saline (pH 7.4) for 15 min each and stained with DAPI (Sigma-Aldrich). Then, sections were mounted on slides for examination under confocal laser scanning microscope (Leica TCS SP5 II). eSLNPs appeared in red due to rhodamine (Excitation 507, Emission 525), whereas the cell nuclei were visualized in blue due to DAPI staining (Excitation 358, Emission 529).

Results and discussion

Physicochemical characterization of NPs: particles size, PDI, and particle zeta potential

In the macroscopic analysis, the dispersion of SLNPs appears with a light, uniform, whitish color, in which the formation of agglomerates is not seen. In addition, the colloidal dispersion shows stability throughout the study. Both eSLNPs and SLNPs with different concentrations of DP were prepared following the previous detailed synthesis method. The results corresponding to the analysis of its size and charge are presented in Table 1.

As can seem in Table 1, the SLNPs have an appropriate size to be injected systemically and be used as pharmaceutical preparation; in this sense, SLNPs with a size between 100 and 200 nm are easily captured by endocytosis, and particles >300 nm are captured by phagocytosis (Decuzzi et al. 2009); therefore, both eSLNP and DP-loaded SLNP should have an ideal size below 300 nm. In fact, the SLNP size is a critical feature to allow it crossing the BBB (Curtis et al. 2018). In fact, as have been published, the interval from 100 to 300nm are the most adequate (Decuzzi et al. 2009), being the optimal size for reaching brain cells around 200nm (Liu and Zhang 2019). The size of SLNPs can be quite varied depending on their nature, and they can be anywhere ranging from 50 to 1000nm in diameter (Ganesan and Narayanasamy 2017); the size, however, can be controlled via various synthesis techniques (Kumar et al. 2018; Sawtarie et al. 2017).

The eSLNPs elaborated without DP had an approximate size of 200 nm; in relation to the NPs loaded with DP, the values obtained, as can be seen in Table 1, were quite similar among them, increasing till 325 nm in the most diluted concentration of DP. The SLNPs loaded with DP resulted in sizes above 200nm, with the exception of the SLNPs that contained the highest concentrated formulation of DP. This may be due to the fact that DP slightly affects the size of the samples, specifically in the process of synthesis, in which the size of the SLNPs would be altered by the drug (Calija 2017).

The PDI were also analyzed for all samples. All measurements show a unimodal curve around the average size obtained. The polydispersity is around 0.3, which is considered quite correct. In the case of the SLNPs with the lowest concentration of DP, the polydispersity values are slightly larger, reaching 0.495, which could also be related to their bigger size. The data obtained in polydispersion are the result of the materials used and the energy used in the sonification process (inversely related) (Tapeinos et al. 2017). In addition, the data reflect the stability of the SLNPs and they are crucial when analyzing their degradation and release kinetics (Busatto et al. 2018).

The ζ-potential is an indicator of the colloidal stability of a system (Wuttke et al. 2017). A ζ-potential with a greater absolute value creates stability in the preparation (Dave et al. 2019). It also becomes a fundamental parameter to cross cell membranes and particularly the BBB; this is due to the presence of proteoglycans, mucopolysaccharides, glycolipids, flucoproteins, sulfates, and sialic acids, all of which give the cell endothelial membrane a negative charge at physiological pH. Thus, electrostatic interaction between the positively charged part of the SLNPs and the negatively charged of the cell membrane could favor its absorption and transportation through the endothelial cells, facilitating its arrival to the brain parenchyma (Çetin et al. 2017).

In the case of our SLNPs, very similar values are presented for all preparations. All of them have a positive charge, as can be seen in Table 1, with an approximate average of 60mV. The empty SLNPs without DP present a higher ζ-potential value, and they decrease slightly in all preparations as DP concentration decrease. In both cases, its positive charge will facilitate internalization compared to neutral or negative charges (Jo et al. 2015).

TEM and SEM analysis

Empty SLNPs were photographed with SEM and TEM microscopy to ascertain its shape as well as to compare with the size data obtained in previous techniques.

Table 1 Average values of size, polydispersion, and zeta potential of NPs studied

	eSLNP(no DA)	SLNP DA 0,2% (w/v)	SLNP DA 0,1% (w/v)	SLNP DA 0,05% (w/v)	SLNP DA 0,03% (w/v)
Size average (nm)	200.1 ± 3.821	174.8 ± 14.4	273.1 ± 15.22	275.0 ± 9.237	325.5 ± 12.86
Polydispersion	0.31 ± 0.03	0.30 ± 0.07	0.29 ± 0.1	0.404 ± 0.03	0.495 ± 0.05
ζ-potentials (mV)	+68.2 ± 1.85	+66.5 ± 2.5	+54.4 ± 1.44	+54.9 ± 1.27	+57.4 ± 1.25

Figure 1a shows the SLNPs in SEM microscopy. Large clusters formed by the accumulation of SLNPs are visible. These aggregates may be due both to the treatment for visualization by microscopy and to the high concentration of SLNPs (Chantaburanan et al. 2017), since the polydispersity and size measurements show a high stability parameter. These SLNPs have a spherical and slightly oval shape, with a smooth surface, and their size is within the parameters analyzed in Table 1. Homogeneity in sizes is evident. Figure 1b focuses on a single SLNP by TEM microscopy. It has a spherical shape and an approximate equivalent size to the data of the previous zetasizer.

The initial spherical shape of these NPs is due, among other things, to the polysorbate 80 which acts as an emulsifier (Sjöström et al. 1995). Variations have been observed with respect to the original spherical shape, with the SLNPs tending to adopt an oval shape due, on the one hand, to the beam of light used in SEM and TEM that can deform the particles and even melt them, and on the other hand, due to polymorphism phenomena (Gordillo-Galeano and Mora-Huertas 2018).

Stability of dopamine

Table 2 presents the averages of the results obtained for stability of DP in the different samples and based on temperature and time. All samples began with a solution of DP in water with a concentration of 0.034mg/mL. This concentration was chosen based on its correspondence with the lowest concentration used in the synthesis of NPs.

In Table 2, it can be observed how both time and temperature play a crucial role in the loss of DP. The oxidation is the main process by which DP is lost (Sánchez-Rivera et al. 2003), and it is evidenced in sample A, which was kept at a temperature of 4°C for 24 h and a week and demonstrates less degradation than samples B and C, which were stored at 25°C at the same times. Light also plays an important role in the oxidation of molecules due to the energy contribution of photons. However, the results of samples B and C are very similar both at 24 h and after 1 week. It is worth mentioning that in samples B and C, which were kept at 25°C, the DP is practically completely degraded after a week.

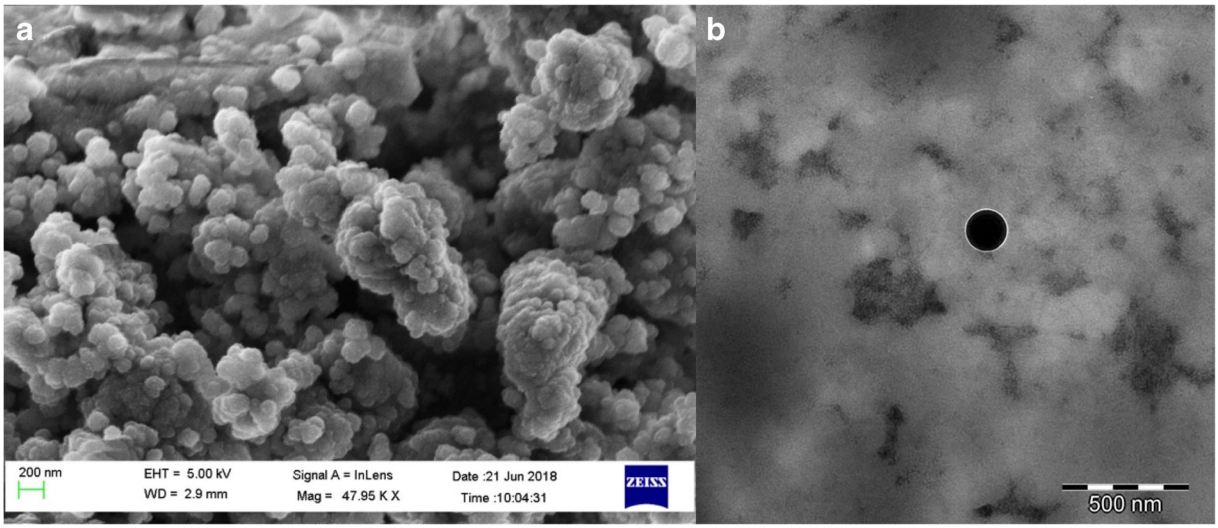

Fig. 1 Empty NPs. **a** SEM. **b** TEM

Table 2 Percentage of lost dopamine for the different simples (A: 4°C and absence light, B: 25°C and absence light, C: 25°C and presence light)

Time	Sample	Percentage of lost dopamine (%)
24 h	A	4.8% ± 0.40%
	B	7.6% ± 0.31%
	C	7.5% ± 0.34%
1 week	A	28.9% ± 1.57%
	B	97.5% ± 0.91%
	C	98.4% ± 1.22%

In contrast, the effect of pH is no significant difference in different dopamine samples, although if it is observed that this slightly decreases the amount of dopamine added is higher. There is no difference in pH after a week of synthesis

Determination of drug encapsulation efficiency (DEE, %)

The amount of drug that can be encapsulated in SLNPs is one of the crucial parameters when determining the dose necessary to obtain the desired effect. The encapsulation should be as large as possible to decrease the amount of formulation administered.

Figure 2 shows the average values corresponding to the encapsulation for the different concentrations of DP assayed. For our study, we considered studying concentrations of around 0.12 mg/mL due to previous revisions (Pahuja et al. 2015). Since it is not administered directly in humans, there is no definite specific dose.

It can be seen that the level of every encapsulation is above 60%, reaching the maximum encapsulation at a concentration of 0.05 mg/mL where it reaches almost a 70% encapsulation. This value is quite good considering the hydrophilic nature of DP. In addition, this is attributable to the synthesis process by the method of emulsification by ultrasonication. In the field of SLNPs %, DEE is a good value, and other authors achieve successful encapsulations with 63% (Pillay et al. 2009).

In vitro dopamine release

The drug release pattern is a very important parameter for any study concerning drug delivery carriers, including lipid SLNPs. Figure 3 shows the percentages of DP released over 168 h.

In the first time frame from 0 to 6 h, the release occurs quickly. This may be due to the rapid dissolution of the existing DP in the areas closest to the surface of the SLNPs (Ganesan and Narayanasamy 2017). Then the curve becomes flatter and the release becomes more

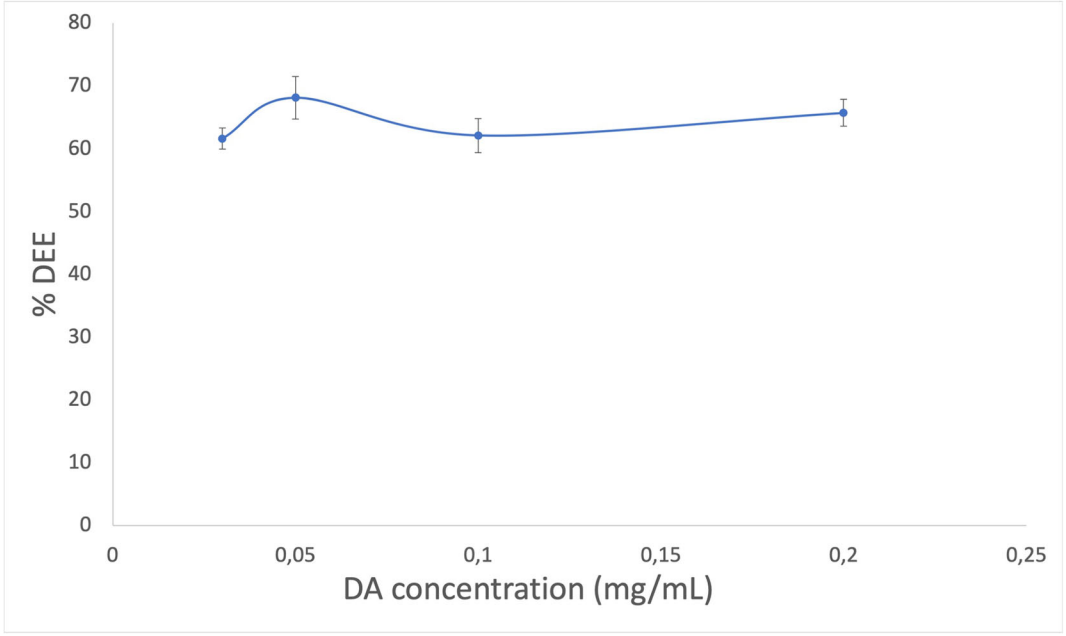

Fig. 2 Percentages of encapsulation for the different DP concentrations

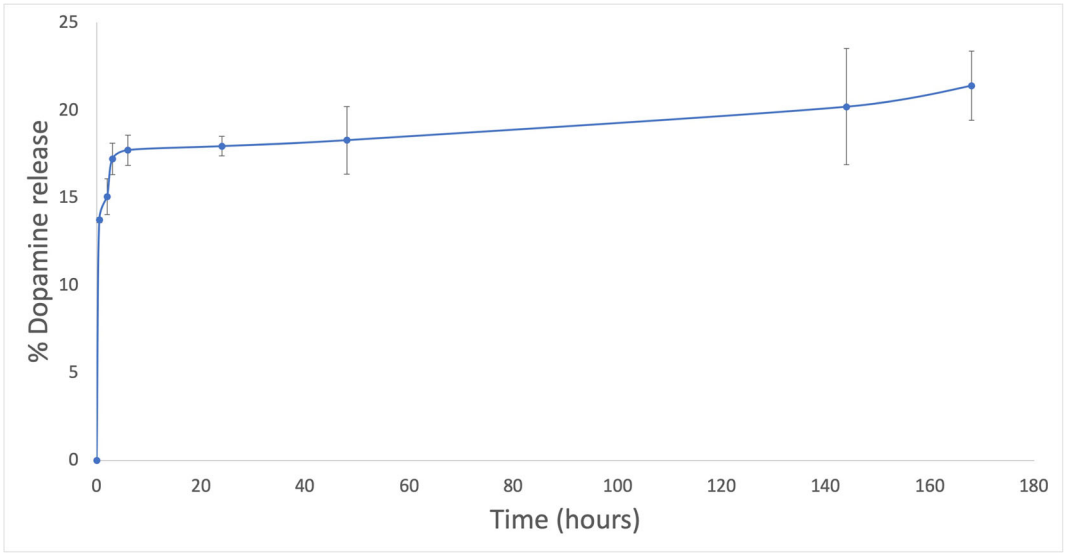

Fig. 3 Percentages of dopamine released over time

sustained over time. The results in this time period from 6 to 168 h are only increased by 4 points. This may be due to the degradation of DP. In the stability study, it can be seen that the concentration of DP decreased with temperature, playing this variable a fundamental role. In this experiment, the temperature is 37°C, which could explain the release of most of the DP and its subsequent degradation, so that, we only come to appreciate 20% of its release when it is already completed.

The experimental data has been adjusted to each of the mathematical methods using the Akaike discriminatory criterion (AIC), in which the method with the lowest AIC value best explains the diffusion process. Table 3 shows the AIC values for the different formulations.

The lowest value is presented by the square root kinetics. This type of kinetics is adjusted to drugs formulated in modified release systems or semi-solid pharmaceutical forms. In both cases, the amount of drug differed as a function of time is determined by the application of the Higuchi equation:

Table 3 Release kinetics of DP SLNPs

Order 1	Higuchi	Hixon-Crowell	Order 0
71.87 ± 2.69	53.46 ± 1.88	64.89 ± 1.07	73.13 ± 1.82

$$Q = \sqrt{(2C_0 - C_s)C_s * D(t - t_0)}$$

in which

D is the drug diffusion coefficient
C_0 The initial amount of drug per unit volume of the matrix
C_s the solubility of the drug in the matrix

This model shows that liberation is not constant, but is time dependent. It will be modified with the square root of time. This type of kinetics is typical of inert matrix systems in which we have a drug and polymer mixtures homogeneously. From that matrix, the drug is released by diffusion. As the molecules inside the matrix must travel a longer path out of the matrix than the shallower molecules, it is why it modifies the release with the square root of time.

Estimation of rhodamine fluorescence of e-SPNPs in the cerebral parenchyma

As observed under confocal microscope (Fig. 4), the empty SLNPs are able to cross the BBB; they appear as red vesicles due to the rhodamine fluorescence within the cerebral parenchyma. Despite the short time elapsed since the injection of the SLNPs (2 h), they can be observed inside the

cytoplasm of the nervous cells, probably associated with the endomembrane cellular system (Fig. 4a); however, some of them are still detected in the lumen of the vessels and inside the vascular wall (Fig. 4b).

Different receptors in endothelial cells could be involved in the mechanisms responsible for the capture of the SLNPs to be transported through the BBB to the brain parenchyma (Alyautdin et al. 2014; Trapani et al. 2011). Nevertheless, these mechanisms are not yet fully known, so more research in this field will be require in the future (Pardridge 2015; Alyautdin et al. 2014).

Conclusions

- The SLNPs loaded with concentrations of DP between 0.2 and 0.05% have sizes below 300nm being suitable for penetration through the blood-brain barrier.
- The surface charges of the SLNP were positive in all cases; these values endorse the stability of the dispersion and favor the internalization into cells.
- SLNPs show a spherical shape, and the DP release is sustained over time resulting adequate to be used as pharmaceutical preparation.

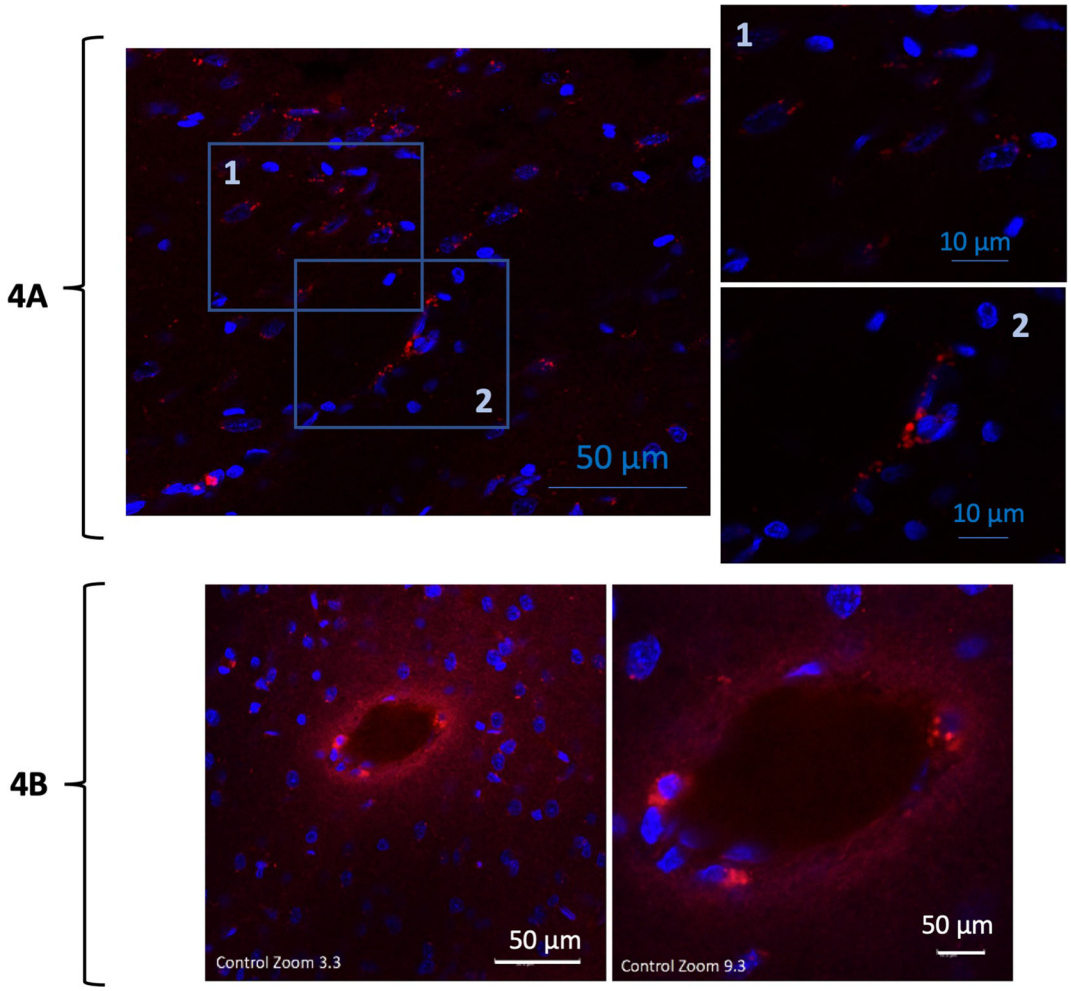

Fig. 4 Confocal microphotographs of a brain sections showing the rhodamine fluorescent eSLNPs in the cerebral parenchyma. **a** The SLNPs as red vesicles inside the nervous cells (probably neurons) (1) and in the vasculature (2). **b** SLNPs inside the vascular wall and also in nervous cells

- At the concentrations studied, the encapsulation concentrations were around 60%.
- SLNPs are able to reach the brain, proving the ability to cross the blood brain barrier.

Author contribution Elena Ortega and Santos Blanco contributed equally to the present work and share first authorship.

Funding We received financial support from project BFU2016-80316-R of Ministerio de Economía y Competitividad (MEC).

Declarations

Conflict of interest The authors declare no competing interests.

References

Alyautdin R, Khalin I, Nafeeza MI, Haron MH, Kuznetsov D (2014) Nanoscale drug delivery systems and the blood–brain barrier. Int J Nanomedicine 9:795–811

Busatto C, Pesoa J, Helbling I, Luna J, Estenoz D (2018) Effect of particle size, polydispersity and polymer degradation on progesterone release from PLGA microparticles: Experimental and mathematical modeling. Int J Pharm 536:360–369

Calija B (2017) Microsized and nanosized carriers or nonsteroidal anti-inflamatory drugs. Formulation Challenges and Potential Benefits. Belgrade, Elservier. Academic Press

Çetin M, Aytekin E, Yavuz B, Bozdag S (2017). Nanoscience in targeted brain drug delivery. nanotechnology methods for neurological diseases and brain tumors. Elservier. 117–147

Chantaburanan T, Teeranachaideekul V, Chantasart D, Jintapattanakit A, Junyaprasert VB (2017) Effect of binary solid lipid matrix of wax and triglyceride on lipid crystallinity, drug-lipid interaction and drug release of ibuprofen-loaded solid lipid nanoparticles (SLN) for dermal delivery. J Colloid Interface Sci 504:247–256

Curtis C, Toghani D, Wong B, Nance E (2018) Colloidal stability as a determinant of nanoparticle behavior in the brain. Colloids Surf B: Biointerfaces 170:673–682

Dave V, Tak K, Sohgaura A, Gupta A, Sadhu V, Reddy KR (2019) Lipid-polymer hybrid nanoparticles: Synthesis strategies and biomedical applications. J Microbiol Methods 160: 130–142

Decuzzi P, Pasqualini R, Arap W, Ferrari M (2009) Expert Review: Intravascular Delivery of particulate systems: does geometry really matter? Pharm Res 26(1):235–243

Doménech Berrozpe J, Martínez Lanao J, Peraire Guitart J et al (eds) (2013) Tratado general de Biofarmacia y Farmacocinética. Vol II. Ed Síntesis, Madrid

Ellis JM, Fell MJ (2017) Current approaches to the treatment of Parkinson's Disease. Bioorg Med Chem Lett 17:4247–4255

Ganesan P, Narayanasamy D (2017) Lipid nanoparticles: Different preparation techniques, characterization, hurdles, and strategies for the production of solid lipid nanoparticles and nanostructured lipid carriers for oral drug delivery. Sustain Chem Pharm 6:37–56

Ghasemiyeh P, Mohammadi-samani S (2018) Solid lipid nanoparticles and nanostructured lipid carriers as novel drug delivery systems: applications, advantages and disadvantages. Res Pharm Sci 13(4):288–303

Gordillo-Galeano A, Mora-Huertas CE (2018) Solid lipid nanoparticles and nanostructured lipid carriers: a review emphasizing on particle structure and drug release. Eur J Pharm Biopharm 133:285–308

Jo DH, Ki JH, Lee TG, Kim JH (2015) Size, surface charge, and shape determine therapeutic effects of nanoparticles on brain and retinal diseases. Nanomedicine 11:1603–1611

Kakadia P, Conway BR (2015) Lipid nanoparticles for dermal drug deliver. Curr Pharm Des 21(20):2823–2829

Kumar R, Singh A, Garg N, Siril PF (2018) Solid lipid nanoparticles for the controlled delivery of poorly water soluble nonsteroidal anti-inflammatory drugs. Ultrason Sonochem 40: 686–696

Kuo Y, Rajesh R (2018) Current development of nanocarrier delivery systems for Parkinson's disease pharmacotherapy. J Taiwan Inst Chem Eng 87:15–25

Liu Q, Zhang Q (2019) 10 - Nanoparticle systems for nose-to-brain delivery. Brain Target Deliv Syst:219–238

Masserini M (2013) Nanoparticles for Brain Drug Delivery. ISRN Biochem 238428:1–18

Naskar S, Sharma S, Kuotsu K (2019) Chitosan-based nanoparticles: an overview of biomedical applications and its preparation. J Drug Deliv Sc Technol 49:66–81

Niu X, Chen J, Gao J (2019) Nanocarriers as a powerful vehicle to overcome blood-brain barrier in treating neurodegenerative diseases: Focus on recent advances. Asian J Pharm Sci 14: 480–496

Pahuja R, Seth K, Shukla A, Shukla RK, Bhatnagar P (2015) Trans-blood brain barrier delivery of dopamine-loaded nanoparticles reverses functional deficits in Parkinsonian rats. ACS Nano 9(5):4850–4871

Pardridge WM (2012) Drug transport across the blood – brain barrier. J Cereb Blood Flow Metab 32:1959–1972

Pardridge WM (2015) Blood–brain barrier endogenous transporters as therapeutic targets: a new model for small molecule CNS drug discovery. Expert Opin Ther Targets 19:1059–1072

Pillay S, Pillay V, Choonara YE, Naidoo D, Khan RA, Toit LC, Ndesendo VNK, Modi G, Danckwerts MP, Iyuke SE (2009) Design, biometric simulation and optimization of a nano-enabled scaffold device for enhanced delivery of dopamine to the brain. Int J Pharm 382:277–290

Portet S (2020) A primer on model selection using the Akaike Information Criterion. Infect Dis Model 5(5):111–128

Rehman M, Madni A, Shi D, Ihsan A, Tahir N, Chang KR, Javed I, Webster IJ (2013) Enhanced blood brain barrier permeability and glioblastoma cell targeting via thermoresponsive lipid nanoparticles. Nanoscale. 9:15434–15440

Sánchez-Rivera AE, Corona-Avendaño S, Alarcón-Angeles G, Rojas-Hernández A, Ramirez-Silva MT, Romero-Romo MA (2003) Spectrophotometric study on the stability of dopamine and the determination of its acidity constants.

Spectrochim Acta Part A Mol Biomol Spectrosc 59(13): 3193–3203

Sawtarie M, Cai Y, Lapitsky Y (2017) Preparation of chitosan/tripolyphosphate nanoparticles with highly tunable size and low polydispersity. Colloids Surf B: Biointerfaces 157:110–117

Sjöström B, Kaplun A, Talmon Y, Cabane B (1995) Nanoparticles prepared in water in oil microemulsion. Pharm Res 12:39–48

Tapeinos C, Battaglini M, Ciofani G (2017) Advances in the design of solid lipid nanoparticles and nanostructured lipid carriers for targeting brain diseases. J Control Release 264: 306–332

Tian C, Asghar S, Xu Y, Chen Z, Zhang J, Ping Q, Xiao Y (2018) Tween 80-modified hyaluronic acid-ss-curcumin micelles for targeting glioma: Synthesis, characterization and their in vitro evaluation. Int J Biol Macromol 120:2579–2588

Trapani A, De Glio E, Cafagna D, Denora N, Agrimi G, Cassano T, Gaetani S, Cuomo V, Trapani G (2011) Characterization and evaluation of chitosan nanoparticles for dopamine brain delivery. Int J Pharm 419(1):296–307

Wuttke S, Lismont M, Escudero A, Rungtaweevoranit B, Parak WJ (2017) Biomaterials Positioning metal-organic framework nanoparticles within the context of drug delivery e A comparison with mesoporous silica nanoparticles and dendrimers. Biomaterials. 123:172–183

Zhou Y, Peng Z, Seven ES, Leblanc RM (2018) Crossing the blood-brain barrier with nanoparticles. J Control Release 270:290–303